

EMISSION SPECTRUM OF A κ -CYGNID METEOR AFTERGLOW. F. Espartero^{1,2}, J.M. Madiedo^{1,3}.
¹Facultad de Ciencias Experimentales, Universidad de Huelva, Huelva, Spain. ²Observatorio Astronómico de Andalucía, 23688 La Pedriza, Alcalá la Real, Jaén, Spain. ³Departamento de Física Atomica, Molecular y Nuclear. Universidad de Sevilla. 41012 Sevilla, Spain.

Introduction: Bright fireballs, specially those moving at high velocity, may produce long-lasting glows called persistent trains. These phenomena can be visible for several minutes after the meteor has disappeared. Once it is formed, the luminosity of the persistent train falls quickly within a few seconds during the so-called afterglow phase.

Meteor spectroscopy is a fundamental technique to get data about the physicochemical composition in meteoric plasmas, and also to get an insight about the chemical composition of meteoroids ablating in the atmosphere. Besides, the analysis of fireball afterglow spectra can provide useful information about the physical processes taking place in persistent meteor trains. However these afterglow spectra are not abundant in the literature (see e.g. [1, 2, 3, 4]). Despite the κ -Cygids do not move at very high speeds, bright κ -Cygids meteors tend to exhibit a final flare as a consequence of the sudden disruption of the progenitor meteoroid when the particle enters denser atmospheric regions. On 15 August 2012 at 23h44m59.7s UTC, a κ -Cygid fireball with an absolute magnitude of -10.5 ± 0.5 was simultaneously imaged from two meteor observing stations located in the South of Spain. The event reached its maximum luminosity during a very bright flare that took place by the end of its atmospheric path, giving rise to a persistent train. The emission spectrum of the meteoric afterglow was recorded during about 0.7 seconds. Here we focus on the analysis of this spectrum afterglow.

Instrumentation and methods: The fireball discussed here was imaged from two meteor observing stations located in the South of Spain (Sevilla and El Arenosillo). These stations employ an array of low-lux monochrome CCD cameras (models 902H2 and 902H Ultimate, manufactured by Watec Co.) that generate interlaced video imagery at 25 frames per second (fps) with a resolution of 720x576 pixels. Full details about the operation of this array of video cameras are given in [5, 6]. For data reduction the AMALTHEA software was employed [7], which calculated the fireball atmospheric trajectory, radiant position and meteoroid orbital data by following the methods described in [8]. On the other hand, to obtain meteor spectra holographic diffraction gratings (with 1000 grooves/mm) are attached to the objective lens of some of the CCD video cameras that operate at the above-mentioned stations. These slitless videospectrographs operate in the framework of the SMART Project, which was

started in 2006 [9]. The spectra are analyzed with the CHIMET software [9].

Observations: According to our calculations, the meteoroid impacted the atmosphere with a velocity $V_\infty = 27.3 \pm 0.3 \text{ km s}^{-1}$ and with an inclination of 26.4° with respect to the local vertical. The fireball began at $109.7 \pm 0.5 \text{ km}$ above the sea level, and ended at a height of $72.0 \pm 0.7 \text{ km}$. By the end of the atmospheric trajectory it exhibited a bright flare. At this stage the event reached its maximum luminosity, which corresponded to an absolute magnitude of -10.5 ± 0.5 . The orbital data of the meteoroid are listed in Table 1. The geocentric radiant was located at $\alpha_g = 291.5 \pm 0.3$, $\delta_g = 60.6 \pm 0.2$. These data confirm the association of this event with the κ -Cygid meteoroid stream.

a (AU)	2.70±0.13	ω ($^\circ$)	199.7±0.3
e	0.634±0.017	Ω ($^\circ$)	143.35399±10 ⁻⁵
q (AU)	0.9895±0.0007	i ($^\circ$)	41.0±0.4

Table 1. Orbital data (J2000).

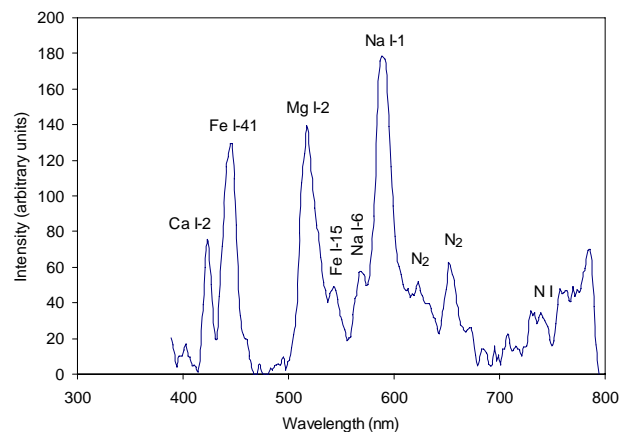


Figure 1. Calibrated afterglow spectrum at $t=0.34 \text{ s}$ after the formation of the persistent train.

Afterglow spectrum: Figure 1 shows the afterglow spectrum at $t = 0.34 \text{ s}$ after the formation of the persistent train. The spectrum, which was recorded for 0.7 s, covered the range between 400 and 800 nm. This signal was calibrated in wavelength and corrected for the spectral sensitivity of the recording device by following the same technique employed for the fireball spectrum. The most important contributions in the afterglow spectrum correspond to multiplets Na I-1 (588.9 nm), Mg I-2 (517.2 nm), Fe I-41 (441.5 nm)

and Ca I-2 (422.6 nm). The emissions due to Fe I-15 (543.4 nm) and Na I-6 (568.8 nm) were also identified, together with several N₂ and N I atmospheric contributions between 600 and 800 nm. The relative intensity of the main emission lines in the calibrated afterglow spectrum (those of multiplets Na I-1 (588.9 nm), Mg I-2 (517.2 nm), Ca I-2 (422.6 nm) and Fe I-41 (441.5 nm)) were measured. Their dependence with time (Figure 2) suggests an exponential decay of the relative intensity I of these lines:

$$I = I_0 \exp(B \cdot t) \quad (1)$$

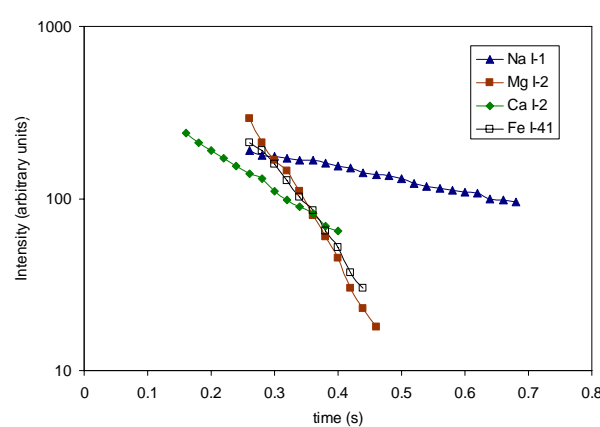


Figure 2. Evolution with time of the relative brightness of the main emission lines identified in the afterglow spectrum.

By fitting these intensities to this equation we have obtained the values of the parameters I_0 and B (Table 2). The parameter B , which measures the decay rate, decreases as the excitation potential E_k increases. This behaviour suggests that the observed decrease in luminosity in these emission lines in the afterglow spectrum is mainly controlled by a temperature-driven mechanism in the meteor train [1]. The fact that the decay is faster for higher values of E_k is also shown in Figure 3, which suggests that this dependence can be described, within the experimental uncertainty, by means of a linear equation:

$$B = B_0 + D E_k \quad (2)$$

where D is the so-called cooling constant. By fitting the values of B in Table 4 to Eq. (2), we obtain $B_0 = 5.7 \text{ s}^{-1}$ and $D = -3.6 \text{ s}^{-1} \text{ eV}^{-1}$. The value of D was found to be of $-1.5 \text{ s}^{-1} \text{ eV}^{-1}$ for a mag. -13 Leonid fireball [1], and $-2.7 \text{ s}^{-1} \text{ eV}^{-1}$ for two additional mag. -8 Leonid bolides [2]. So, the cooling was faster in the persistent train of the κ -Cygnid analyzed here than in the persistent train of the above-mentioned Leonids.

Multiplet	λ (nm)	E_k (eV)	I_0 (a.u.)	B (s ⁻¹)
Na I-1	588.9	2.10	291 ± 4	-1.6 ± 0.3
Ca I-2	422.6	2.93	566 ± 10	-5.4 ± 0.4
Fe I-41	441.5	4.41	2950 ± 420	-9.9 ± 0.5
Mg I-2	517.2	5.10	8183 ± 1023	-12.9 ± 0.4

Table 2. Calculated values of the parameters in Eq. (1) for the main emission lines identified in the afterglow spectrum. The excitation potential of the upper level (E_k) is included.

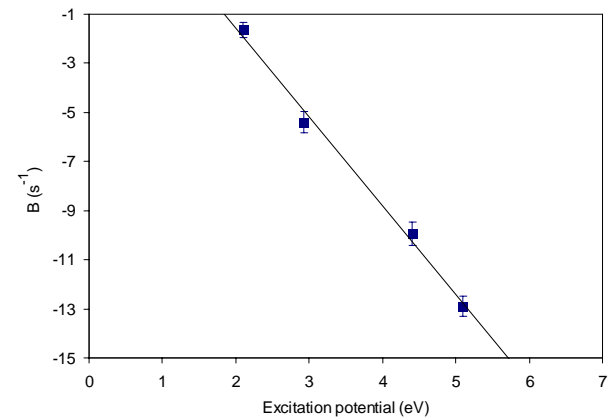


Figure 3. Dependence of the decay exponent B in Eq. (1) on the excitation potential. The solid line corresponds to the fit given by Eq. (2).

Conclusions: The analysis of the double-station fireball discussed here has provided the atmospheric trajectory and radiant of the bolide and the heliocentric orbit of the progenitor meteoroid. These data reveal that this particle belonged to the κ -Cygnid meteoroid stream. The fireball reached its maximum brightness during a bright flare that took place by the end of its atmospheric path, reaching an absolute magnitude of -10.5 ± 0.5 . Several emission lines produced by Na, Mg, Ca and Fe were identified in the afterglow emission spectrum, which could be recorded for about 0.7 seconds. The brightness of the emission lines of Na I-1, Fe I-41, Ca I-2 and Mg I-2 was found to decrease exponentially with time. The observations suggest that this decrease in luminosity is mainly controlled by a temperature-driven mechanism in the meteor train.

References: [1] Borovička J. and Jenniskens P., 2000, *Earth Moon Planets*, 8283, 399. [2] Abe S. et al., 2005, *Earth Moon Planets*, 95, 265. [3] Jenniskens P. et al., 2000, *Earth Moon Planets*, 82-83, 429-438. [4] Madiedo J.M. et al., 2014, *A&A*, 569, A104. [5] Madiedo J.M. and Trigo-Rodríguez J.M. (2008) *EMP* 102, 133-139. [6] Madiedo J.M. et al. (2010) *Adv.in Astron*, 2010, 1-5. [7] Madiedo J.M. et al. (2011), *NASA/CP-2011-216469*, 330. [8] Ceplecha Z., 1987, *Bull. Astron. Inst. Cz.* 38, 222-234. [9] Madiedo J.M., 2014, *Earth, Planets and Space*, 66, 70.